Organic & Biomolecular Chemistry

ROYAL SOCIETY OF CHEMISTRY

PAPER

View Article Online
View Journal | View Issue

Cite this: *Org. Biomol. Chem.*, 2020, **18**, 3104

Synthesis, radiolabelling and initial biological characterisation of ^{18}F-labelled xanthine derivatives for PET imaging of Eph receptors†‡

Marc Pretze, §¶[a,b] Christin Neuber, §[a] Elisa Kinski,[a] Birgit Belter,[a] Martin Köckerling, [c] Amedeo Caflisch, [d] Jörg Steinbach, [a,b] Jens Pietzsch [a,b] and Constantin Mamat *[a,b]

Eph receptor tyrosine kinases, particularly EphA2 and EphB4, represent promising candidates for molecular imaging due to their essential role in cancer progression and therapy resistance. Xanthine derivatives were identified to be potent Eph receptor inhibitors with IC_{50} values in the low nanomolar range (1–40 nm). These compounds occupy the hydrophobic pocket of the ATP-binding site in the kinase domain. Based on lead compound **1**, we designed two fluorine-18-labelled receptor tyrosine kinase inhibitors (**[^{18}F]2/3**) as potential tracers for positron emission tomography (PET). Docking into the ATP-binding site allowed us to find the best position for radiolabelling. The replacement of the methyl group at the uracil residue (**[^{18}F]3**) rather than the methyl group of the phenoxy moiety (**[^{18}F]2**) by a fluoropropyl group was predicted to preserve the affinity of the lead compound **1**. Herein, we point out a synthesis route to **[^{18}F]2** and **[^{18}F]3** and the respective tosylate precursors as well as a labelling procedure to insert fluorine-18. After radiolabelling, both radiotracers were obtained in approximately 5% radiochemical yield with high radiochemical purity (>98%) and a molar activity of >10 GBq μmol^{-1}. In line with the docking studies, first cell experiments revealed specific, time-dependent binding and uptake of **[^{18}F]3** to EphA2 and EphB4-overexpressing A375 human melanoma cells, whereas **[^{18}F]2** did not accumulate at these cells. Since both tracers **[^{18}F]3** and **[^{18}F]2** are stable in rat blood, the novel radiotracers might be suitable for *in vivo* molecular imaging of Eph receptors with PET.

Received 22nd February 2020,
Accepted 31st March 2020

DOI: 10.1039/d0ob00391c

rsc.li/obc

Introduction

The Eph (erythropoietin-producing hepatoma cell line) receptor family represents the largest subfamily of receptor tyrosine kinases and, at present, comprises 14 members divided into two groups, A and B.[1] Their corresponding, membrane-attached (GPI-anchored) ephrin A and (transmembrane located) ephrin B ligands bind to the Eph receptors in a juxtacrine manner which provides the condition for Eph receptor forward and ephrin reverse signaling.[2]

Eph receptors and their ephrin ligands play a crucial role during embryogenesis by regulating spatial patterning, vascular development, and axon guidance.[3,4] Moreover, the Eph/ephrin system is involved in tissue homeostasis, for instance of bone, intestine, and the immune system.[5,6] All these effects are based on the regulation of cell–cell communication as well as cell attachment, shape, and motility by Eph receptors and their ephrin ligands.[7]

Beside their role during developmental processes it became evident that the Eph/ephrin system plays an important role in the pathogenesis of many diseases.[5] In this regard, Eph receptors are often dysregulated in cancer, whereby expression can be both up and down regulated.[8] Eph receptors can act both as tumour promotor and tumour suppressor, depending, *e.g.*, on the cellular context, ligand stimulation, and the kind of result-

[a]*Helmholtz-Zentrum Dresden-Rossendorf, Institut für Radiopharmazeutische Krebsforschung, Bautzner Landstraße 400, D-01328 Dresden, Germany. E-mail: c.mamat@hzdr.de*
[b]*Technische Universität Dresden, Fakultät Chemie und Lebensmittelchemie, D-01062 Dresden, Germany*
[c]*Universität Rostock, Institut für Chemie – Anorganische Festkörperchemie, Albert-Einstein-Straße 3a, D-18059 Rostock, Germany*
[d]*Department of Biochemistry, University of Zurich, Winterthurerstrasse 190, CH-8057 Zurich, Switzerland*

†Dedicated to the memory of Prof. Rudolf Münze (Central Institute for Nuclear Research Rossendorf, Germany), deceased in February 2020.

‡Electronic supplementary information (ESI) available: NMR spectra of compounds. CCDC 1976810 and 1976126. For ESI and crystallographic data in CIF or other electronic format see DOI: 10.1039/d0ob00391c

§These authors contributed equally to this work.

¶Current address: Klinik und Poliklinik für Nuklearmedizin, Universitätsklinikum Carl Gustav Carus der TU Dresden, Fetscherstraße 74, D-01307 Dresden, Germany.

ing signaling crosstalk.[8,9] In particular, EphA2 and EphB4 receptors are highly expressed in a number of tumour entities, including breast, prostate, lung, and ovarian cancer, and are often associated with poor prognosis[8,10] as well as therapy resistance.[11,12] In brief, EphA2 receptor induces proliferation, migration, and invasion of tumour cells, resulting in higher tumourigenicity and enhanced tumour vascularisation.[1,13] EphB4 and its cognate ligand ephrin B2, by contrast, affect tumour growth mostly by regulation of tumour angiogenesis and vascular remodelling, which also may result in an unfavourable tumour microenvironment, *e.g.* hypoxia.[14–16] In line with this, EphB4 has been linked to tumour therapy resistance, for instance when using the DNA damaging agent cisplatin or the VEGF targeting antibody bevacizumab.[17,18] Therefore, they are emerging targets for the functional characterisation of tumours by non-invasive molecular imaging purposes like positron emission tomography (PET) or single photon emission computed tomography (SPECT), and the derivation of corresponding therapeutic applications.

In light of the involvement of the Eph/ephrin system in several pathologies including cancer, a wide range of agents targeting Eph receptors and their corresponding ephrins arose in the last years. To date, several potent Eph kinase inhibitors are reported in the literature either based on biomacromolecules like peptides,[19–21] which bind to the extracellular ligand binding domain of the appropriate receptor, or based on small organic molecules,[22] which are able to block the intracellular ATP-binding pocket. Selected compounds were chosen to be radiolabelled with either technetium-99m[23] for SPECT or with copper-64[24] and fluorine-18[25] like peptide **I**[26] as well as with carbon-11 like derivative **IIIa**[27] for PET (Scheme 1).

In the past, we developed the fluorine-18-containing radiotracers **IIb**[28] based on the benzodioxolylpyrimidine structural motif and **IIIb**[29] containing the indazolylpyrimidine core. Compound **IIb** showed a substantial uptake in human melanoma cells (A375) *in vitro* but no uptake in the corresponding melanoma xenograft model *in vivo* despite of the high affinity of the original compounds to the EphB4 receptor. These results prompted us to search for an improved lead structure. In this regard, compound **1** (designated as compound **3** in ref. 30) containing a xanthine skeleton published by Nevado in 2009 and 2013 was chosen as lead compound.[30,31] For lead compound **1**, a high affinity in the low nanomolar range (1–40 nm) was described for 10 Eph receptors including EphA2 and EphB4, the two receptors which are mainly involved in cancer progression and therapy resistance.

In the present paper, a synthesis route to two novel fluorine-18-containing derivatives ([^{18}F]**2**/**3**) of lead compound **1** and the respective precursors for radiolabelling as well as a labelling procedure to insert fluorine-18 is presented. Prior to synthesis and radiolabelling, *in silico* docking studies were accomplished to find the best position for labelling with fluorine-18. Based on these results first *in vitro* experiments were performed to investigate both binding behavior to EphA2 and EphB4 overexpressing human A375 melanoma cells and metabolic stability.

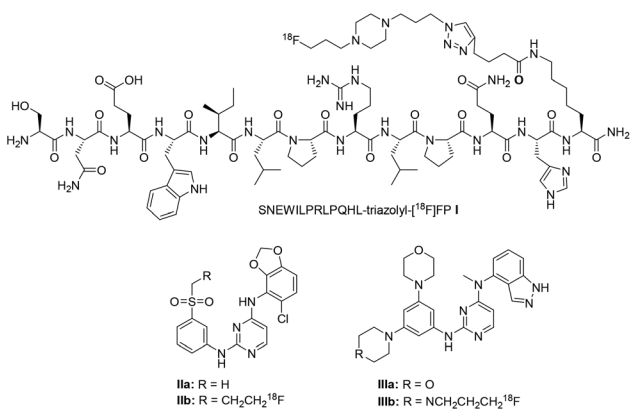

Scheme 1 Structures of ^{11}C- and ^{18}F-labelled radiotracers **I**–**III** based on Eph inhibitors prepared by our group.

Results

In silico design

As most of the pharmaceuticals in clinical use do not contain fluorine, an isosteric radiolabelling with fluorine-18 is not possible if these molecules are also interesting for molecular imaging. Instead of this, single hydrogen atoms or functional groups like hydroxy groups are typically replaced by fluorine-18.[32] However, this replacement can lead to a change in the pharmacological behavior of the compounds. Thus, the search of an acceptable labelling position is mandatory and can be performed by docking studies, particularly, if the (holo) structure of the target protein has been reported.

The chosen lead compound **1**, containing a xanthine skeleton, has been published by the group of Nevado.[30] To investigate local selectivity (inhibitory activity on a single branch of the kinome dendrogram), lead compound **1** was tested by an enzymatic assay with [γ-^{33}P]ATP against a panel of 11 Eph receptor kinases. Due to the high sequence identity of Eph receptors (60–90%) and their small gatekeeper residue threonine in the ATP-binding site, compound **1** showed IC_{50} values in the nanomolar range for nearly all Eph receptors (IC_{50}: 2.9 nM (EphA1), 2.3 nM (EphA2), 3.3 nM (EphA4), 3.0 nM (EphA5), 4.5 nM (EphA8), 1.1 nM (EphB1), 1.2 nM (EphB2), and 1.6 nM (EphB4)).[30] In general, the size of the gatekeeper residue of the hydrophobic pocket of the ATP-binding site determines affinity as well as selectivity of RTK inhibitors.[33] Both EphA2 and EphB4 belong to the subfamily of kinases (~20% of the 518 human kinases) with a small (threonine) gatekeeper (Thr693).

Moreover, compound **1** was tested for its global selectivity (inhibitory activity on the whole kinome) and was shown to strongly inhibit six further kinases (out of 85 tested), namely Src, Lck, Yes1, CSK, BTK, and HER-4, which all have a threonine gatekeeper.[30] Overall, lead compound **1** showed high inhibition against 21 out of 143 tested kinases, about half of

which were chosen because of their small gatekeeper residue, and 10 of them are Eph kinases.

Explicit solvent molecular dynamics simulations of the complex of the kinase domain and a precursor of lead compound **1** (compound **3** in ref. 30), had revealed involvement of carbonyl C_6=O and amide group N_1–H in hydrogen bonds with the backbone polar groups of Met696 of EphB4.[30] For the development of the two novel ^{18}F-based radiotracers [^{18}F]**2** and [^{18}F]**3**, we decided to choose two sites of the original inhibitor that are not directly involved in binding interactions. Radiotracers [^{18}F]**2** and [^{18}F]**3** are based on the replacement of a methyl group by a fluoropropyl group at the phenoxy moiety and uracil residue of the lead compound **1**, respectively (Scheme 2). Advantageously, the fluoropropyl moiety is less sterically hindered and has a comparable *in vivo* stability as fluoroethyl, but it is much more stable compared to the fluoromethyl residue.[34,35]

Starting from the crystal structure of compound **1** in the complex with the kinase domain (PDB code 4GK2), manual docking of the two derivatives was carried out with the program WITNOTP, which is available from the homepage of one of the authors (AC). The docking of compound **2** resulted in steric clashes of the propyl chain with the N-terminal or C-terminal domain of the kinase depending on the orientation of the phenyl ring. In contrast, the fluorinated propyl residue of compound **3** could be accommodated without steric conflicts as it points towards the exposed region of the ATP-binding site (Fig. 1).

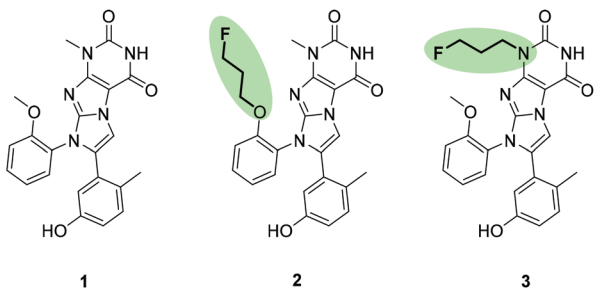

Scheme 2 Literature known lead compound **1** and proposed structures of fluorine-containing-compounds **2** and **3** with highlighted labelling positions.

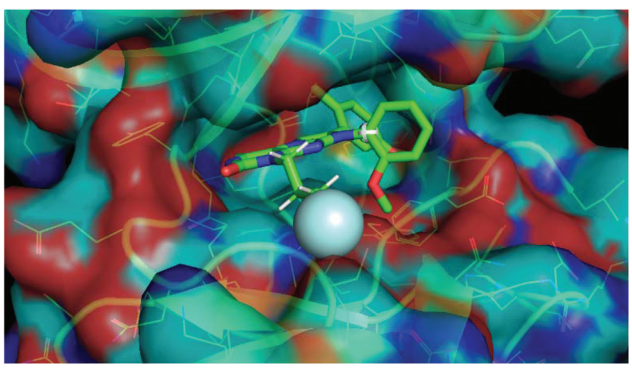

Fig. 1 Predicted binding mode of compound **3** in the ATP-binding site of the EphA3 receptor. The position of the fluorine atom is emphasised by a cyan sphere and hydrogen atoms are shown only for the propyl chain.

Chemistry

N-Modified aminouracils were applied as basis for the preparation of the original lead compound **1**, both ^{18}F-radiotracers [^{18}F]**2,3**, the non-radioactive reference compounds **2,3** and their respective precursors **14a,b**. In the first step, unsymmetrically alkylated urea derivatives **4a–c** were prepared from the respective amines and sodium cyanate.[36] Next, compounds **4a–c** were reacted with ethyl 2-cyanoacetate and sodium ethanolate in a Traube purine synthesis[37] to the *N*-substituted uracil derivatives **5a–c**. The preparation of the bromoxanthins was accomplished according to the literature.[30] For this purpose, all three uracil derivatives **5a–c** were treated with $NaNO_2$ under acidic conditions which resulted in the nitroso derivatives **6a–c** (yields: 79–83%). Next, the diamino compounds **7a–c** were prepared by the reduction of **6a–c** with sodium dithionite. Due to the instability of the free diamines, compounds **7a–c** were subsequently converted into the respective xanthines **8a–c** by treatment with triethyl orthoformate and *p*-TsOH. The last step required the insertion of bromine. Therefore, **8a–c** were treated with elemental bromine for 3 h at 65 °C. Bromo derivatives **9a–c** were obtained in high yields of 74–84%. The whole reaction sequence to the brominated xanthines starting from the appropriate ureas is shown in Scheme 3.

During the synthesis of the urea derivatives **4a–c** and the bromo xanthines **9a–c**, it was possible to obtain single crystals of **4b** and **9a** suitable for single crystal X-ray analyses. The molecular structures of **4b** and **9a** are presented in Fig. 2 and 3, respectively.

The compound **4b** crystallises in the monoclinic and **9a** in the triclinic crystal system. The structures confirm the identities of the two compounds and the correctness of the reaction pathways. All bond distances in both structures are within the expected ranges. In crystals of **4b**, the molecules are arranged

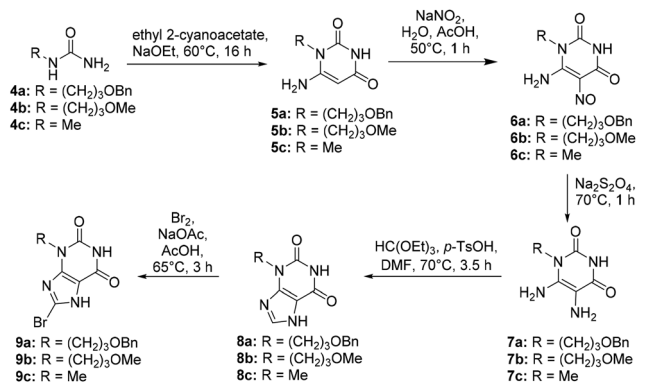

Scheme 3 Reaction sequence to brominated xanthine derivatives **9a–c** starting from urea derivatives **4a–c**.

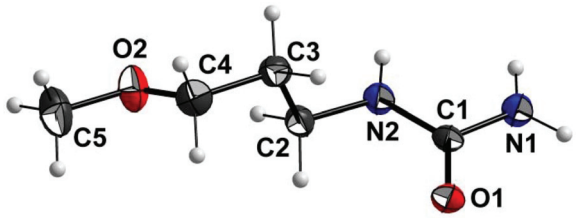

Fig. 2 Molecular structure of **4b** in the crystal with atom labelling scheme (ORTEP plot, 50% probability level).

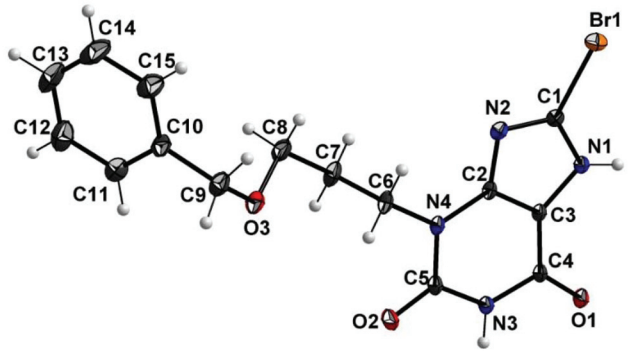

Fig. 3 Molecular structure of **9a** in the crystal with atom labelling scheme (ORTEP plot, 50% probability level).

such that hydrogen bonds are formed between the NH_2 group (around N1) and the O1 atoms of neighbouring molecules at distances of 2.927(1), 2.948(1), and 3.033(1) Å. In crystals of **9a** the molecules are arranged, such that the xanthine units as well as the phenyl rings of the benzyl group are arranged parallel to same units of neighboring molecules, but outside of distances of π–π-interactions. Hydrogen bonds exist between the H atoms of both NH groups (N1 and N3) to O1 and O2, respectively, of neighboring molecules at distances of 2.6875 (9) and 2.817(1) Å.

The next reaction sequence to obtain the final compounds started with the synthesis of 2-bromo-1-(5-hydroxy-2-methylphenyl)ethanone (**10**),[30] which was then connected to xanthines **9a–c**. The desired compounds **11a–c** were obtained in nearly quantitative yields of >99%. At this stage, the benzylgroup of **11a** as well as the methyl group of **11b** were inevitable to be cleaved with BBr_3 in dichloromethane to give **11d** (yield: 99% starting from **11a** and 84% starting from **11b**). The final cyclisation reaction of **11c,d** with alkoxyanilines **12a,b** to the imidazopurinediones **13a–c** was accomplished under Lewis acid catalysis ($AlCl_3$), which is important for the success of the reaction. Otherwise, only open-chained products were obtained.[38] The synthesis was executed either with 2-methoxyaniline (**12a**) and **9c** to yield **13a** (62%) or with 2-(3-hydroxypropoxy)aniline (**12b**) and **11b** to give **13b** (83% yield). A further optimisation consisted in the application of four equivalents of the respective aniline derivative (**12a** or **12b**). In addition, the original inhibitor **13c** was also obtained by the reaction of **11c** with 2-methoxyaniline (**12a**) in a yield of 88%.

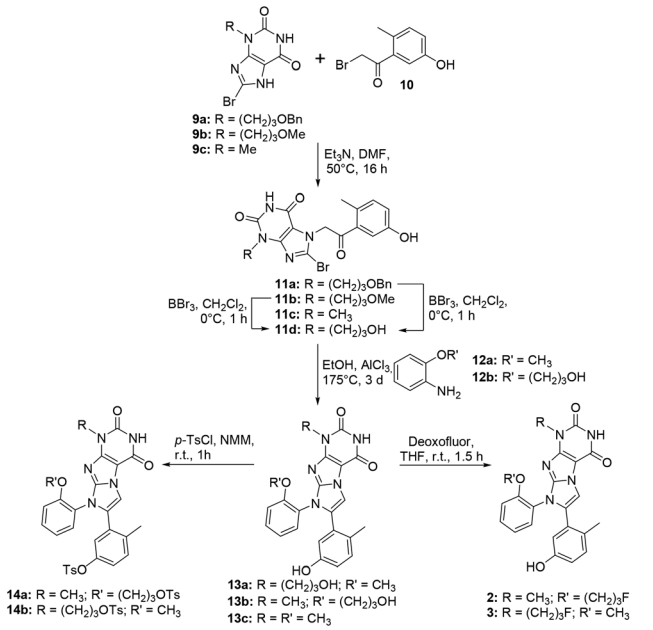

Scheme 4 Reaction sequence to the fluorinated reference compounds **2,3** and their tosylated precursors **14a,b**.

The full reaction sequence to the final compounds is shown in Scheme 4.

The last step to prepare the non-radioactive reference compounds **2** and **3** involved the introduction of fluorine into **13a, b**. Attempts to use **14a,b** for a nucleophilic introduction of fluoride were not successful. Alternatively, hydroxy compound **13a** was treated with Deoxofluor in anhydrous THF under ambient temperature for 1 h which led to reference compound **3** in a yield of 10%. The second reference compound was synthesised from **13b** with DAST which led to **2** in a yield of 80%. Treatment of **13a,b** with *p*-TsCl in *N*-methylmorpholine yielded the desired precursors **14a** (96%) and **14b** (77%) for the later radiolabelling procedure. The use of DMF as solvent should be avoided due to the formation of unexpected by-products.[39]

Radiolabelling

The radiosyntheses of both radiotracers [^{18}F]**2** and [^{18}F]**3** were achieved in a one-step procedure by classical aliphatic nucleophilic substitution of the tosylate group in precursors **14a,b** with n.c.a. [^{18}F]fluoride as shown in Scheme 5. Necessarily, the tosyl group attached to the phenyl moiety of **14a,b** has to be cleaved simultaneously. Labelling conditions were optimised for [^{18}F]**2** with regard to various reaction parameters such as solvent, reaction temperature, synthesis time, and also in combination with microwave (mw) conditions.

The use of [^{18}F]TBAF in *t*-butanol[40] and acetonitrile under standard heating and mw conditions (15 and 30 W) for 10 min showed no conversion. When using 70 W for 10 min, a new spot was detected on the TLC with a R_f value of 0.55 (solvent: chloroform/MeOH = 9/1, silica gel), but not at the R_f value of the reference compound **2** (R_f = 0.37). The more lipophilic spot

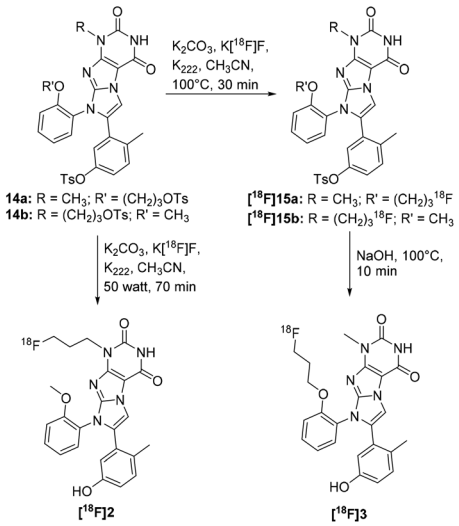

Scheme 5 Radiolabelling procedure for the synthesis of tracers [^{18}F]**2** and [^{18}F]**3**.

indicated the still tosyl group-containing tracer [^{18}F]**15a** of approx. 5%.

The use of K[^{18}F]F/K_{222}/K_2CO_3 mixture in acetonitrile at room temperature yielded the spot at R_f = 0.55 as well and a very weak spot at R_f = 0.37. Finally, the use of mw conditions (10 min, 30 W) with the afore mentioned labelling conditions was successful and delivered a spot for the desired product at R_f = 0.37. An elongation of 40 min at 50 W delivered the tracer [^{18}F]**2** in 10% RCY and tosylated [^{18}F]**15a** in <2% RCY (Fig. 4). Finally, after 70 min at 50 W only the desired product [^{18}F]**2** was detected in 13% RCY (Table 1 and Fig. 5). The unusual long labelling time is related to the cleavage of the second tosyl group of the former precursor molecule, which occurred as well under these conditions, but very slowly in comparison to the radiofluorination step. Thus, the by-products [^{18}F]**15a,b**, still containing the tosyl group bound to the phenol unit, were

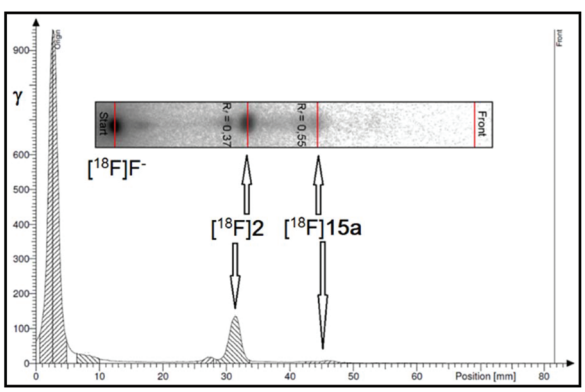

Fig. 4 Radiolabelling of [^{18}F]**2**: radio-TLC analysis (eluent: $CHCl_3$: MeOH 9 : 1), [^{18}F]**2** (R_f = 0.37) and [^{18}F]**15a** (R_f = 0.55) after 40 min at 50 watt.

Table 1 Evaluation of the labelling conditions used for [^{18}F]**2**

Entry	Conditions	Heating	Time	[^{18}F]**15**	[^{18}F]**2**
1	[^{18}F]TBAF, CH_3CN[a]	rt	60 min	0	0
2	[^{18}F]TBAF, CH_3CN[a]	30 W	10 min	0	0
3	[^{18}F]TBAF, CH_3CN	70 W	60 min	5	0
4	K[^{18}F]F, K_{222}, K_2CO_3, CH_3CN	rt	10 min	2	Trace
5	K[^{18}F]F, K_{222}, K_2CO_3, CH_3CN	30 W	10 min	5	2
6	K[^{18}F]F, K_{222}, K_2CO_3, CH_3CN	50 W	40 min	<2	10
7	K[^{18}F]F, K_{222}, K_2CO_3, CH_3CN	50 W	70 min	0	13
8	K[^{18}F]F, K_{222}, K_2CO_3, CH_3CN	100 W	10 min	Dec.	Dec.

[a] *tert*-BuOH was tested as well

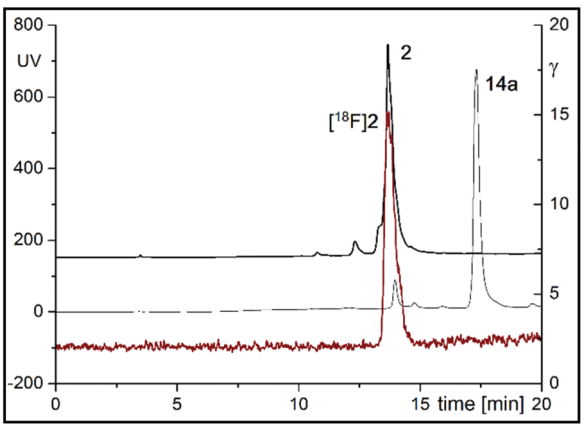

Fig. 5 (Radio-)HPLC chromatograms of purified [^{18}F]**2** (γ-trace: red line, t_R = 13.7 min), reference compound **2** (UV-trace: bold black line, t_R = 13.7 min) and precursor **14a** (UV-trace: black line, t_R = 17.4 min).

first formed and then [^{18}F]**2/3** after an elongation of the reaction time.

The purification of [^{18}F]**2** was executed using two Chromafix® C18 cartridges. For this purpose, the reaction mixture was diluted with deionised water and the resulting solution was transferred to the cartridges. The first elution was done with deionised water to remove remaining [^{18}F]fluoride. The still trapped [^{18}F]**2** was eluted with MeOH and then finally purified using semipreparative HPLC to obtain 21–69 MBq (1–6% d.c.) RCY with a A_m = 10.3 ± 5.1 GBq μmol^{-1}. Radio-TLC and radio-HPLC analyses showed no other radioactive by-products (Fig. 5). Radiotracer [^{18}F]**3** was prepared *via* a two step procedure. First, the aliphatic tosylate group was converted under standard radiofluorination conditions using K_{222}, K_2CO_3 and [^{18}F]F$^-$ at 100 °C for 30 min, whereas the aromatic tosylate was not affected. Afterwards, aqueous NaOH was added and the mixture was again heated at 100 °C for 15 min to cleave the remaining aromatic tosyl group. Purification was done *via* semi-preparative HPLC to obtain [^{18}F]**3** in RCYs between 3–5%.

Radiopharmacological investigations

To give a first impression of the later (radio-)pharmacological behavior of the radiofluorinated tracers, log *P*(*D*) values were calculated and compared with the experimentally determined values for the fluorinated compounds **2** and **3** as well as the lead compound **1** using ChemDraw and ACD labs (Table 2). Experimental determination using the shake flask method revealed suitable log *P* values of 2.2 and 2.9 for compound **2** and **3**, respectively, which are comparable with the log *P* value of the lead compound **1**.

Cellular binding and uptake of [^{18}F]**2** and [^{18}F]**3** was accomplished using A375 melanoma cells with low Eph receptor expression (A375) as well as transfected A375-EphA2 and A375-EphB4 cells, which are characterised by a substantial increased expression of EphA2 and EphB4, respectively (Fig. 6A).

Cellular binding and uptake of radiotracer [^{18}F]**2** was lower than the uptake of [^{18}F]**3** resulting in less and more than 50% ID mg^{-1} (injected dose per mg protein), respectively (Fig. 6B/C). With regard to [^{18}F]**2** there was no difference in cellular tracer binding and uptake between non-transfected A375 cells and A375-EphA2 or A375-EphB4 cells (Fig. 6B). The missing increase of tracer binding and uptake by time may result from a lack in Eph receptor affinity and/or an active tracer efflux due to activity of multi drug resistance (MDR) proteins like P-glycoprotein (P-gp). With regard to the latter, Lafleur *et al.* already recognised that compound **1** is a substrate for P-gp transporters, since inhibitory activity of compound **1** decreased by almost two orders of magnitude when investigating IC_{50} in EphB4-overexpressing cells instead of by using recombinant protein (130 nM in cellular assay *vs.* 5 nM in enzymatic assay) as a result of efficient substrate efflux.[31] In contrast to [^{18}F]**2**, cellular binding and uptake of [^{18}F]**3** was remarkably increased in A375-EphA2 and A375-EphB4 cells in comparison to A375 cells, amounting up to 110 and 90% ID mg^{-1}, respectively (Fig. 6C).

The specificity of radiotracer uptake was tested by performing blocking experiments with all three cell lines after pre-incubation with lead compound **1** or the non-radioactive reference compound **2**. Cellular binding and uptake of [^{18}F]**2** in A375-EphA2 cells could be significantly blocked by pre-incubation with compound **2** (100 μM) at all investigated time points, whereas tracer accumulation in A375-EphB4 cells could be blocked only after 120 min (Fig. 6D). Pre-incubation with lead compound **1** (50 μM) significantly decreased tracer accumulation in all three cell lines at 30, 60, and 120 min (Fig. 6E). With regard to this, it has to be kept in mind that lead compound **1** showed IC_{50} values in the low nanomolar range (1–40 nM) against almost all Eph receptors due to their high sequence identity (60–90%) and their small gatekeeper residue (threonine) of the hydrophobic pocket of their ATP-binding site.[13] Since we could demonstrate mRNA expression of EphA1–4, EphA7, and EphB1-B4 in A375 cells in a previous study,[48] this might be the reason for the inhibition of radiotracer binding and uptake even in non-transfected A375 cells.

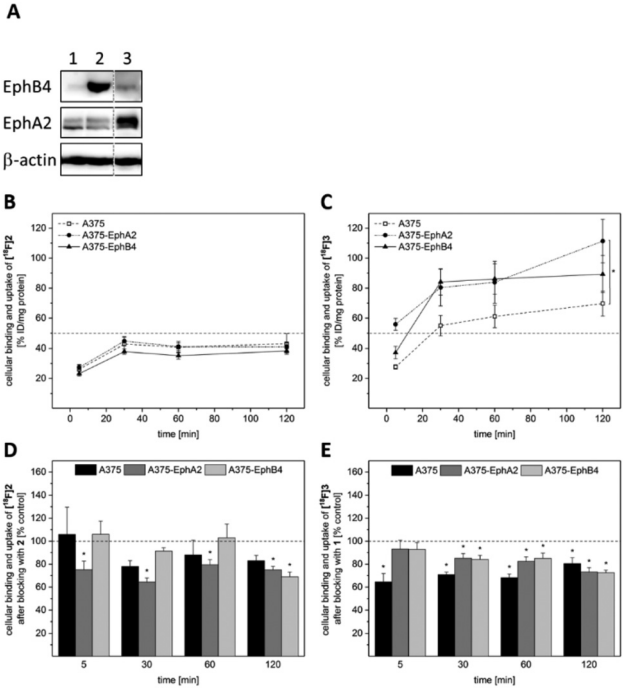

Fig. 6 Cellular binding and uptake of radiotracer [^{18}F]**2** and [^{18}F]**3** over a period of 120 min at 37 °C in non-transfected as well as EphA2- and EphB4-transfected A375 melanoma cells. (A) Representative Western blots for EphA2 and EphB4 in (1) A375, (2) A375-EphB4, and (3) A375-EphA2 cells. (B/C) Cellular binding and uptake of radiotracers [^{18}F]**2** and [^{18}F]**3** in A375, A375-EphA2, and A375-EphB4 cells after 5, 30, 60, and 120 min at 37 °C. (D/E) For blocking experiments, cellular binding and uptake of radiotracers [^{18}F]**2** and [^{18}F]**3** was investigated in all three cell lines after pre-incubation with compound **2** and lead compound **1**, respectively. Values represent mean ± standard deviation (SD) from at least two independent experiments each performed in quadruplicate.

First *in vitro* stability tests were accomplished with [^{18}F]**2** and [^{18}F]**3** in rat blood and plasma at 37 °C for up to 60 min and analysed *via* radio-TLC and radio-HPLC. No radiodefluorination or other degradation processes were observed for both [^{18}F]**2** and [^{18}F]**3** within at least 60 min. Further *in vivo* metabolite analyses using rats showed a fast blood clearance of [^{18}F]**2** and [^{18}F]**3** at 60 min p.i. resulting in radioactivity concentrations insufficient for metabolite analysis by radio-TLC or radio-HPLC. Additionally, a nearly complete degradation of [^{18}F]**2** and [^{18}F]**3**, respectively, to a more hydrophilic metabolite was found in the urine. Exemplarily, PET imaging with [^{18}F]**2** confirmed a very fast blood clearance and elimination *via* hepatobiliary and, of minor importance, *via* renal route even after 5 min p.i. in the rat (Fig. 7).

Table 2 Calculated and determined log *P*(*D*) values for **2**, **3**, and the lead **1**

Compound	Lead **1**	**2**	**3**
Calculated log *P*[41]	2.86	3.16	3.16
Calculated log $D_{(pH\ 7.4)}$[42]	3.04	3.48	3.44
Determined log *P*	—	2.2	2.9

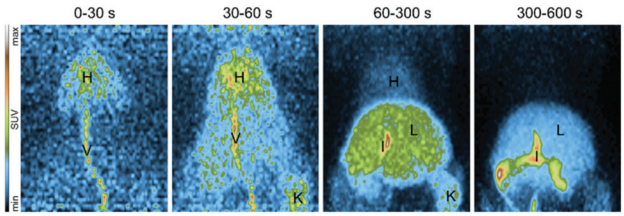

Fig. 7 Representative PET images (MIP, maximum intensity projection) after i.v. injection of [^{18}F]**2** into a rat. To illustrate fast elimination of [^{18}F]**2** MIPs are delineated for different time frames (0–30 s, 30–60 s, 60–300 s, and 300–600 s) up to 10 min p.i. Different organs are marked as H-heart, V-vein, K-kidney, L-liver, I-intestine. Images are depicted at same SUV scale.

Discussion

Due to promiscuity of the Eph/ephrin system and missing selectivity of radiotracers targeting the hydrophobic pocket of the ATP-binding site[43,44] we consciously decided to test a multi-Eph receptor tracer approach by choosing an imidazopurinedione derivative developed by Nevado/Lafleur (lead compound **1**) as lead compound for radiolabelling with fluorine-18. Due to the high sequence identity of Eph receptors (60–90%) and their small gatekeeper residue (threonine) in the hydrophobic pocket of the ATP-binding site, lead compound **1** showed IC_{50} values in low nanomolar range (1–40 nM) against EphA1–5, EphA8, and EphB1–4. For EphA2 and EphB4, which are mainly involved in cancer progression and therapy resistance, IC_{50} values in an enzymatic assay using [γ-^{33}P]ATP were 2.3 nM and 1.6 nM, respectively. Moreover, lead compound **1** was shown to strongly inhibit six further kinases (out of 85 tested), namely Src, Lck, Yes1, CSK, BTK, and HER-4, which all have a threonine gatekeeper.[30]

For purposes of nuclear imaging, especially with PET, we developed two derivatives of lead compound **1**, each bearing a [^{18}F]fluoropropyl side chain instead of a methyl group at the phenoxy ring ([^{18}F]**2**) and uracile ([^{18}F]**3**), respectively. Docking studies suggested a diminished binding potential to the EphB4 receptor for [^{18}F]**2**. However, *in vitro* assay pointed out a high stability of [^{18}F]**2** in rat blood. In first cellular binding and uptake experiments, we could not observe a time-dependent increase in cellular binding and uptake of [^{18}F]**2** in EphA2- or EphB4-overexpressing A375 melanoma cells, which is in line with the docking prediction, but might also be the consequence of MDR protein, *e.g.*, P-gp, mediated tracer efflux. Therefore, we focused on compound [^{18}F]**3**, bearing a [^{18}F] fluoropropyl side chain instead of a methyl group at the uracil residue. Docking experiments predicted a conserved binding affinity for this compound. In line with this, we found an increased cellular binding and uptake of [^{18}F]**3** to A375 melanoma cells overexpressing EphA2 or EphB4. Moreover, blocking with compound **1** revealed specificity of binding. Since this tracer was quite stable in rat blood *in vitro* over 60 min and, therefore, might be suitable for *in vivo* applications, future studies now have to focus on blood clearance rate and metabolic stability *in vivo* to finally assess feasibility of our newly developed radiotracer [^{18}F]**3** for *in vivo* molecular imaging with PET. Such radiotracers may allow (i) for characterisation of tumours and metastasis with regard to their molecular fingerprint and the functional expression of ('drugable') targets and (ii) for monitoring of (early) effects of (Eph) targeted therapies. As an example, an on-going phase I clinical trial (NCT03374943) is investigating the EphA3-targeting antibody KB004 in patients with recurrent glioblastoma.[45,46] By combining an initial PET imaging sequence using [^{89}Zr]KB004 followed by the therapeutic application of KB004 promising clinical responses in the absence of any dose-limiting toxicities or drug-related side effects have been reported initially. With regard to the approach chosen here, we generally point out that a high degree of selectivity is not always desirable for therapeutic purposes, and that inhibitors targeting multiple kinases, for example, which are involved in tumor angiogenesis or cancer progression, may have an increased efficacy and a better ability to circumvent resistance mechanisms. In quantitative molecular imaging it should be carefully considered whether, for example, multi-Eph targeting is desirable. This depends on the type of tumor under investigation and its molecular fingerprint, especially with regard to the up- or down-regulation of the individual Eph receptors. A very selective tracer approach can make an important contribution to the identification of exactly this individual molecular fingerprint, which in turn provides important information on the response to therapy.

Experimental

Materials and methods

All reagents were purchased from commercial suppliers and were used without further purification. Compounds **4b–7b** were prepared according to van Muijlwijk-Koezen *et al.*[44] and compounds **4c–13c** were prepared according to Lafleur *et al.*[30] Analytical TLC was performed on pre-coated Silica Gel 60 F_{254} plates (Merck) and results read under UV-light (λ = 254 nm). ^{1}H NMR, ^{13}C NMR and ^{19}F NMR spectra were recorded on a Varian Inova-400 or an Agilent 400-DD2 spectrometer with ProbeOne at 400, 101, and 376 MHz, respectively. Chemical shifts are reported in ppm with tetramethylsilane (^{1}H, ^{13}C) and trichlorofluoromethane (^{19}F) as internal standard, respectively. MS spectra were obtained on a Micromass Quattro-LC spectrometer using electron spray (ESI) as ionisation method. Melting points were recorded on a Cambridge Instruments Galen III apparatus and are uncorrected. Single-crystal X-ray diffraction data of **4b** (CCDC 1976810) and **9a** (CCDC 1976126)‡ were collected with a Bruker-Nonius Apex-X8 CCD-diffractometer using graphite-monochromated MoK_{α} radiation (λ = 0.71073 Å). The diffraction measurements were done at −150 °C. The structures were solved by Direct Methods and refined against F^2 on all data by full-matrix least-squares using the sHELX suite of programs.[47] All non-hydrogen atoms were refined anisotropically; all hydrogen atoms bound to C atoms were placed on cal-

culated positions and refined using a riding model. Final *R* values converged at *R*1 = 0.035 (**4b**) and *R*1 = 0.030 (**9a**). Analytical HPLC was performed on a VWR/Hitachi Elite La Chrome HPLC system, equipped with a reverse phase column (Nucleosil 100-5C18 Nautilus), a UV-diode array detector (254 nm) and a scintillation radiodetector (Raytest, Gabi Star) at a flow rate of 1 mL min^{-1} (eluent: acetonitrile/water, 30 : 70 + 0.1% TFA). The radioactive compound was identified using analytical radio-HPLC by comparison of the retention time t_R of the reference compound. Semi-preparative radio-HPLC was performed on a Jasco HPLC system (Nucleosil Standard C18 100 Å 7μ, Macherey-Nagel, 250 × 16 mm, eluent: CH_3CN/H_2O + 0.1% TFA/0 → 1 min: 90% H_2O, 1 → 18 min: 90% → 10% H_2O, 18 → 25 min: 10% H_2O, flow rate: 4 mL min^{-1}). Decay-corrected RCYs were quantified by integration of radioactive peaks on a radio-TLC using a radio-TLC scanner (Fuji, BAS2000). [^{18}F]fluoride was produced by the $^{18}O(p,n)^{18}F$ nuclear reaction utilizing the PET cyclotron Cyclone 18/9 (IBA, Belgium) by irradiation of [^{18}O]H_2O.

Synthetic procedures

1-(3-(Benzyloxy)propyl)urea (4a). Under Ar, 1-(3-(benzyloxy) propan-1-amine (2.35 g, 14.22 mmol) was dissolved in water (10 mL) and NaNCO (1.11 g, 17.07 mmol) was added in five portions within 10 min. Afterwards, the mixture was heated at 100 °C for 30 min, cooled to rt and was allowed to stand overnight. The precipitated product (scratch with glas rod) was filtered and washed with a small amount of cold water to give **4a** as colorless solid (1.10 g, 37%); mp 80–82 °C; R_f = 0.44 (ethyl acetate : MeOH = 6 : 1); ^{1}H NMR (400 MHz, $CDCl_3$): δ 7.40–7.27 (m, 5H, H_{Ar}), 4.99 (br s, 1H, NH), 4.61 (br s, 2H, NH_2), 4.49 (s, 2H, CH_2Ph), 3.58 (t, ^3J = 5.7 Hz, 2H, NCH_2), 3.28 (t, ^3J = 6.1 Hz, 2H, OCH_2), 1.83–1.77 (m, 2H, CH_2) ppm; ^{13}C NMR (101 MHz, $CDCl_3$): δ 158.8 (C═O), 138.1 (C-i), 128.5 (C-m), 127.8 (C-p), 127.7 (C-o), 73.1 (CH_2Ph), 68.5 (OCH_2), 38.8 (NCH_2), 29.7 (CH_2) ppm; MS (ESI+): *m*/*z* 231 (M^+ + Na, 100%), 209 (M^+ + H, 35).

6-Amino-1-(3-(benzyloxy)propyl)pyrimidine-2,4(1*H*,3*H*)-dione (5a). Elemental sodium (1.86 g, 80.7 mmol) was dissolved in absolute EtOH (100 mL) and **4a** (5.6 g, 53.8 mmol) and ethyl cyanoacetate (6.09 g, 53.8 mmol) were added to this solution and the resulting mixture was heated to 60 °C for 16 h. An organge precipitate appeared which disappeared after addition of conc. HCl to pH ≈ 3 under formation of a colorless precipitate. This was filtered and washed with EtOH (10 mL) and ethyl acetate (20 mL). The solvent was removed and the remaining residue was purified *via* column chromatography (ethyl acetate → ethyl acetate : EtOH = 10 : 1) and **5a** was obtained as bright yellow solid (3.8 g, 51%); mp 171–173 °C; R_f = 0.30 (ethyl acetate : EtOH = 6 : 1); ^{1}H NMR (400 MHz, DMSO-d_6): δ 10.30 (s, 1H, NH), 7.37–7.26 (m, 5H, H_{Ar}), 6.73 (s, 2H, NH_2), 4.53 (s, 1H, CH), 4.44 (s, 2H, CH_2Ph), 3.82 (t, ^3J = 7.3 Hz, 2H, NCH_2), 3.46 (t, ^3J = 6.3 Hz, 2H, OCH_2), 1.83–1.77 (m, 2H, CH_2); ^{13}C NMR (101 MHz, DMSO-d_6): δ 162.2 (C═O), 155.6 (CNH_2), 151.1 (C═O), 138.3 (C-i), 128.1 (C-m), 127.4 (C-o), 127.3 (C-p), 75.4 (CH), 71.8 (CH_2Ph), 67.0 (OCH_2), 38.2 (NCH_2), 27.7 (CH_2) ppm; MS (ESI+): *m*/*z* 298 (M^+ + Na, 40%), 276 (M^+ + H, 30).

6-Amino-1-(3-(benzyloxy)propyl)-5-nitrosopyrimidine-2,4(1*H*,3*H*)-dione (6a). Compound **5a** (1.46 g, 5.30 mmol) was suspended in a mixture of water (30 mL) and acetic acid (12 mL), $NaNO_2$ (548 mg, 7.96 mmol) was added and the mixture was maintained at 50 °C for 1 h and at 4 °C overnight. The resulting purple precipitate was filtered and washed with ice water. The resulting solid was dried at 80 °C for 3 h and compound **6a** was obtained as deep purple solid (1.13 g, 70%); mp 118–120 °C; R_f = 0.34 (ethyl acetate : EtOH = 6 : 1); ^{1}H NMR (400 MHz, DMSO-d_6): δ 13.34 (s, 1H, NH_2), 11.48 (s, 1H, NH), 9.06 (s, 1H, NH_2), 7.35–7.25 (m, 5H, H_{Ar}), 4.42 (s, 2H, CH_2Ph), 3.88 (t, ^3J = 7.2 Hz, 2H, NCH_2), 3.48 (t, ^3J = 6.1 Hz, 2H, OCH_2), 1.83–1.77 (m, 2H, CH_2); ^{13}C NMR (101 MHz, DMSO-d_6): δ 160.3 (C═O), 151.1 (CNH_2), 148.8 (C═O), 138.8 (CN═O), 138.3 (C-i), 128.2 (C-m), 127.5 (C-o), 127.4 (C-p), 71.9 (CH_2Ph), 67.1 (OCH_2), 38.1 (NCH_2), 26.5 (CH_2); MS (ESI+): *m*/*z* 327 (M^+ + Na, 50%), 305 (M^+ + H, 100).

5,6-Diamino-1-(3-(benzyloxy)propyl)pyrimidine-2,4(1*H*,3*H*)-dione hydrochloride (7a). Sodium dithionite (1.14 g, 5.57 mmol) was added portionwise to a suspension of **6a** (1.13 g, 3.71 mmol) in water (20 mL) and the resulting solution was heated at 70 °C for 1 h (the color turned to light-green). Next, the volume of the solution was reduced by half and then cooled. The precipitate was filtered, washed with ice water and the resulting solid was dried at 90 °C for 3 h and compound **7a** was obtained as light-green solid (1.12 g, 99%); mp 261–262 °C (decomp.); R_f = 0.14 (ethyl acetate : MeOH = 2 : 1); ^{1}H NMR (400 MHz, DMSO-d_6): δ 10.53 (s, 1H, NH), 7.37–7.26 (m, 5H, H_{Ar}), 6.09 (s, 2H, NH_2), 4.45 (s, 2H, CH_2Ph), 3.86 (t, ^3J = 7.2 Hz, 2H, NCH_2), 3.47 (t, ^3J = 6.3 Hz, 2H, OCH_2), 2.83 (s, 2H, NH_2), 1.84–1.77 (m, 2H, CH_2) ppm; ^{13}C NMR (101 MHz, DMSO-d_6): δ 159.6 (C═O), 149.3 (CNH_2), 145.4 (C═O), 138.4 (C_{ipso}), 128.2 (C_{meta}), 127.6 (C_{ortho}), 127.4 (C_{para}), 96.3 (NCC═O), 71.9 (CH_2Ph), 67.1 (OCH_2), 30.7 (NCH_2), 28.0 (CH_2). MS (ESI+): *m*/*z* 313 (M^+ + Na, 20%), 291 (M^+ + H, 100). Due to the instability of that compound, it should be immediately converted into its hydrochloride. Thus, the product (1.12 g) was treated with ice-cold HCl (37%, 15 mL) and stirred for 1 h at rt. The HCl was removed under vacuum and the remaining solid dried under vacuum to yield the hydrochloride **7a** as hygroscopic pale red solid (1.27 g, 99%); mp 128–130 °C (decomp.); R_f = 0 (ethyl acetate : MeOH = 2 : 1); ^{1}H NMR (400 MHz, DMSO-d_6): δ 11.14 (s, 1H, NH), 9.31 (s, 3H, NH_3^+), 7.64 (s, 2H, NH_2), 7.37–7.26 (m, 5H, H_{Ar}), 4.44 (s, 2H, CH_2Ph), 3.91 (t, ^3J = 7.2 Hz, 2H, NCH_2), 3.48 (t, ^3J = 6.2 Hz, 2H, OCH_2), 1.84–1.77 (m, 2H, CH_2); ^{13}C NMR (101 MHz, DMSO-d_6): δ 158.7 (C═O), 149.9 (CNH_2), 149.5 (C═O), 138.4 (C_{ipso}), 128.2 (C_{meta}), 127.5 (C_{ortho}), 127.4 (C_{para}), 83.0 (NCC═O), 71.9 (CH_2Ph), 67.0 (OCH_2), 39.5 (NCH_2), 27.6 (CH_2) ppm; MS (ESI+): *m*/*z* 313 (M^+ + Na − HCl, 20%), 291 (M^+ − Cl, 100).

3-(3-(Benzyloxy)propyl)-1*H*-purine-2,6(3*H*,7*H*)-dione (8a). Compound **7a** (2.0 g, 6.12 mmol) was dissolved in anhydrous DMF (30 mL) under an argon atmosphere. Triethyl orthoformiate (2.29 mL, 13.77 mmol) and *p*-toluenesulfonic acid (monohydrate, 150 mg, 0.79 mmol) were added and the mixture was stirred at 70 °C for 3.5 h. After cooling to rt, ice water (10 mL)

was added and the mixture was allowed to crystallise at approx. 4 °C overnight. Next, the solid was filtered and washed with cold water. After drying at 90 °C, compound **8a** was obtained as yellowish solid (76%, 1.4 g); mp 241–242 °C; R_f = 0.51 (ethyl acetate : MeOH = 4 : 1); ^{1}H NMR (400 MHz, DMSO-d_6): δ 13.47 (s, 1H, NHCH), 11.07 (s, 1H, NHC═O), 8.01 (s, 1H, CH), 7.35–7.25 (m, 5H, H_{Ar}), 4.41 (s, 2H, CH_2Ph), 4.03 (t, ^3J = 7.0 Hz, 2H, NCH_2), 3.49 (t, ^3J = 6.1 Hz, 2H, OCH_2), 1.97–1.90 (m, 2H, CH_2) ppm; ^{13}C NMR (101 MHz, DMSO-d_6): δ 154.7 (C═O), 150.8 (C═O), 149.3 (CH), 140.5 (NCN), 138.5 (C-i), 128.2 (C-m), 127.4 (C-o), 127.3 (C-p), 106.9 (NCC═O), 71.9 (CH_2Ph), 67.4 (OCH_2), 39.8 (NCH_2), 27.9 (CH_2) ppm; MS (ESI+): *m*/*z* 323 (M^+ + Na, 40%), 301 (M^+ + H, 100).

3-(3-(Methyloxy)propyl)-1*H*-purine-2,6(3*H*,7*H*)-dione (8b). Compound **7b** (2.56 g, 10.2 mmol) was dissolved in anhydrous DMF (30 mL) under an argon atmosphere. Triethyl orthoformiate (3.66 mL, 22.0 mmol) and *p*-toluenesulfonic acid (monohydrate, 251 mg, 1.32 mmol) were added and the mixture was stirred at 70 °C for 3.5 h. After cooling to rt, ice water (15 mL) was added and the mixture was allowed to crystallise at approx. 4 °C overnight. Next, the solid was filtered and washed with cold water and acetone. After drying, compound **8b** was obtained as yellowish solid (55%, 1.25 g); mp 221 °C; ^{1}H NMR (400 MHz, DMSO-d_6): δ 13.38 (s, 1H, NHCH), 11.03 (s, 1H, NHC═O), 7.98 (s, 1H, CH), 3.98 (t, ^3J = 7.2 Hz, 2H, NCH_2), 3.36 (t, ^3J = 6.2 Hz, 2H, OCH_2), 3.20 (s, 3H, CH_3), 1.83–1.91 (m, 2H, CH_2) ppm; ^{13}C NMR (101 MHz, DMSO-d_6): δ 154.7 (C═O), 150.8 (C═O), 149.3 (CH), 140.6 (NCN), 107.2 (NCC═O), 69.5 (OCH_2), 57.8 (CH_3), 27.8 (CH_2) ppm; MS (ESI+): *m*/*z* 247 (M^+ + Na, 40%), 225 (M^+ + H, 100).

3-(3-(Benzyloxy)propyl)-8-bromo-1*H*-purine-2,6(3*H*,7*H*)-dione (9a). Elemental bromine (144 μL, 2.83 mmol) was added dropwise to a solution of **8a** (710 mg, 2.36 mmol) and NaOAc (321 mg, 4.72 mmol) in glacial acetic acid (25 mL) and the resulting mixture was stirred at 65 °C for 3 h. After cooling to 0 °C, saturated bicarbonate solution (20 mL) was slowly added and the solution extracted with ethyl acetate (3 × 25 mL). The combined organic layers were dried over $MgSO_4$, the solvent was removed and the crude product was recrystalised with a small amount of dichloromethane to obtain **9a** as pale-yellow solid (750 mg, 84%); mp 214–216 °C; R_f = 0.64 (ethyl acetate : MeOH = 4 : 1); ^{1}H NMR (400 MHz, DMSO-d_6): δ 11.16 (s, 1H, NHC═O), 7.35–7.26 (m, 5H, H_{Ar}), 4.41 (s, 2H, CH_2Ph), 3.97 (t, ^3J = 7.0 Hz, 2H, NCH_2), 3.48 (t, ^3J = 6.0 Hz, 2H, OCH_2), 1.95–1.90 (m, 2H, CH_2) ppm; ^{13}C NMR (101 MHz, DMSO-d_6): δ 153.6 (C═O), 150.5 (C═O), 149.3 (CCO), 138.4 (C-i), 128.2 (C-m), 127.5 (C-o), 127.3 (C-p), 124.3 (C_{Br}), 109.6 (NCN), 80.0 (NCC═O), 79.3 (NCN), 71.9 (CH_2Ph), 67.3 (OCH_2), 38.6 (NCH_2), 27.8 (CH_2) ppm; MS (ESI+): *m*/*z* 403 (M^+ + Na, ^{81}Br, 97%), 401 (M^+ + Na, ^{79}Br, 100), 381 (M^+ + H, ^{81}Br, 53), 379 (M^+ + H, ^{79}Br, 55).

3-(3-(Methyloxy)propyl)-8-bromo-1*H*-purine-2,6(3*H*,7*H*)-dione (9b). Elemental bromine (360 μL, 7.08 mmol) was added dropwise to a solution of **8b** (1.25 g, 5.57 mmol) and NaOAc (750 mg, 9.14 mmol) in glacial acetic acid (25 mL) and the resulting mixture was stirred at 65 °C for 3 h. After cooling to 0 °C, saturated bicarbonate solution (20 mL) was slowly added and the solution extracted with ethyl acetate (3 × 25 mL). The combined organic layers were dried over $MgSO_4$, the solvent was removed and the crude product was recrystalised with a small amount of dichloromethane to obtain **9b** as pale-yellow solid (750 mg, 84%); ^{1}H NMR (400 MHz, DMSO-d_6): δ 11.17 (s, 1H, NHC═O), 3.92 (t, ^3J = 7.3 Hz, 2H, NCH_2), 3.35 (t, ^3J = 6.1 Hz, 2H, OCH_2), 3.19 (s, 3H, CH_3), 180–1.89 (m, 2H, CH_2); ^{13}C-NMR (101 MHz, DMSO-d_6): δ 153.7 (C═O), 150.5 (NCC═O), 149.3 (C═O), 124.3 (C_{Br}), 109.6 (NCN), 69.5 (OCH_2), 57.9 (CH_3), 27.7 (CH_2) ppm; MS (ESI+): *m*/*z* 327 (M^+ + Na, ^{81}Br, 97%), 325 (M^+ + Na, ^{79}Br, 100), 305 (M^+ + H, ^{81}Br, 40), 303 (M^+ + H, ^{79}Br, 42).

3-(3-(Benzyloxy)propyl)-8-bromo-7-(2-(5-hydroxy-2-methylphenyl)-2-oxoethyl)-1*H*-purine-2,6(3*H*,7*H*)-dione (11a). Compound **9a** (930 mg, 2.45 mmol) and DIPEA (633 mg, 4.90 mmol) were dissolved in anhydrous DMF (5 mL) and 2-bromo-1-(5-hydroxy-2-methylphenyl)ethanone (**10**, 843 mg, 3.68 mmol) dissolved in DMF (5 mL) was added dropwise and the resulting solution was stirred at 50 °C overnight. Afterwards, the solvent was removed and the crude product was purified using column chromatography (chloroform → chloroform : MeOH = 25 : 1) to obtain **11a** as solid (1.3 g, 99%); mp 172–173 °C; R_f = 0.18 (ethyl acetate); ^{1}H NMR (400 MHz, DMSO-d_6): δ 11.32 (s, 1H, NH), 9.74 (s, 1H, OH), 7.37–7.27 (m, 6H, H_{Ar}), 7.18 (d, $^3J_{3,4}$ = 8.3 Hz, 1H, H-3), 6.96 (dd, $^3J_{3,4}$ = 8.3 Hz, $^4J_{4,6}$ = 2.5 Hz, 1H, H-4), 5.70 (s, 2H, CH_2C═O), 4.43 (s, 2H, CH_2Ph), 4.02 (t, ^3J = 6.9 Hz, 2H, NCH_2), 3.51 (t, ^3J = 6.0 Hz, 2H, OCH_2), 2.29 (s, 3H, CH_3), 1.99–1.91 (m, 2H, CH_2) ppm; ^{13}C NMR (101 MHz, DMSO-d_6): δ 194.1 ($CH_2\underline{C}$═O), 155.4 (C-5), 154.1 (C═O), 150.2 (C═O), 148.7 (NCN), 138.4 (C-i), 134.6 (C-1), 133.0 (C-3), 129.2 (C-2), 128.2 (C-m), 128.0 (C_{Br}), 127.5 (C-o), 127.3 (C-p), 119.7 (C-4), 115.5 (C-6), 109.0 (N$\underline{C}$C═O), 71.9 (CH_2Ph), 67.3 (OCH_2), 54.3 ($\underline{CH_2}$C═O), 39.2 (NCH_2), 27.8 (CH_2), 19.7 (CH_3) ppm; MS (ESI+): *m*/*z* 551 (M^+ + Na, ^{81}Br, 90%), 549 (M^+ + Na, ^{79}Br, 100), 527 (M^+ + H, ^{81}Br, 83), 529 (M^+ + H, ^{79}Br, 80).

3-(3-(Methyloxy)propyl)-8-bromo-7-(2-(5-hydroxy-2-methylphenyl)-2-oxoethyl)-1*H*-purine-2,6(3*H*,7*H*)-dione (11b). Compound **9b** (758 mg, 2.50 mmol) and DIPEA (485 mg, 3.75 mmol) were dissolved in anhydrous DMF (5 mL) and 2-bromo-1-(5-hydroxy-2-methylphenyl)ethanone (**10**, 630 mg, 2.75 mmol) dissolved in DMF (5 mL) was added dropwise and the resulting solution was stirred at 50 °C overnight. Afterwards, the solvent was removed and the crude product was purified using column chromatography (chloroform → chloroform : MeOH = 20 : 1) to obtain **11b** as colorless solid (1.1 g, 97%); mp 213 °C; R_f = 0.38 (chloroform : MeOH = 9 : 1); ^{1}H NMR (400 MHz, DMSO-d_6): δ 11.34 (s, 1H, NH), 9.75 (s, 1H, OH), 7.35 (d, $^3J_{4,6}$ = 2.3 Hz, 1H, H-6), 7.18 (d, $^3J_{3,4}$ = 8.4 Hz, 1H, H-3), 6.96 (dd, $^3J_{3,4}$ = 8.4 Hz, $^4J_{4,6}$ = 2.3 Hz, 1H, H-4), 5.71 (s, 2H, CH_2C═O), 3.97 (t, ^3J = 7.1 Hz, 2H, NCH_2), 3.39 (t, ^3J = 6.0 Hz, 2H, OCH_2), 3.22 (s, 3H, CH_3), 2.28 (s, 3H, CH_3), 1.86–1.92 (m, 2H, CH_2); ^{13}C NMR (101 MHz, DMSO-d_6): δ 194.2 ($CH_2\underline{C}$═O), 155.4 (C-5), 154.1 (C═O), 150.2 (C═O), 148.7 (NCN), 134.6 (C-1), 133.0 (C-3), 129.2 (C-2), 128.0 (C_{Br}), 119.7

(C-4), 115.5 (C-6), 109.0 (NCC=O), 69.5 (OCH_2), 57.9 (OCH_3), 54.3 (CH_2C=O), 39.8 (NCH_2), 27.7 (CH_2), 19.7 (CH_3) ppm; MS (ESI+): *m*/*z* 575 (M + Na, ^{81}Br, 85%), 573 (M^+ + Na, ^{79}Br, 87), 553 (M^+ + H, ^{81}Br, 23), 551 (M^+ + H, ^{79}Br, 25).

8-Bromo-7-(2-(5-hydroxy-2-methylphenyl)-2-oxoethyl)-3-(3-hydroxypropyl)-1*H*-purine-2,6(3*H*,7*H*)-dione (11d). Starting from **11a**: BBr_3 (1 M in CH_2Cl_2, 7.4 mL, 7.36 mmol) was slowly added to a suspension of **11a** (1.38 g, 2.64 mmol) in anhydrous CH_2Cl_2 (20 mL) at 0 °C and the solution was stirred for 1 h at 0 °C. Afterwards, water was added for quenching and the formed precipitate was filtered, washed with CH_2Cl_2 (2 × 10 mL) and water (2 × 10 mL) and dried *in vacuo* to obtain **11d** as colorless solid (1.15 g, 99%). Starting from **11b**: BBr_3 (1 M in CH_2Cl_2, 7.0 mL, 9.96 mmol) was slowly added to a suspension of **11b** (1.0 g, 2.22 mmol) in anhydrous CH_2Cl_2 (20 mL) at 0 °C and the solution was stirred for 1 h at 0 °C. Next, water was added for quenching and the formed precipitate was filtered, washed with CH_2Cl_2 (2 × 10 mL) and water (2 × 10 mL) and dried *in vacuo* to obtain **9d** as colorless solid (813 mg, 84%); mp 229–230 °C; R_f = 0.50 (ethyl acetate : MeOH = 8 : 1); ^{1}H NMR (400 MHz, DMSO-d_6): δ 11.33 (s, 1H, NH), 9.73 (s, 1H, HOPh), 7.35 (d, $^4J_{4,6}$ = 2.5 Hz, 1H, H-6), 7.18 (d, $^3J_{3,4}$ = 8.3 Hz, 1H, H-3), 6.96 (dd, $^3J_{3,4}$ = 8.3 Hz, $^4J_{4,6}$ = 2.5 Hz, 1H, H-4), 5.71 (s, 2H, CH_2C=O), 3.97 (t, ^3J = 7.5 Hz, 2H, NCH_2), 3.51 (t, ^3J = 6.4 Hz, 2H, OCH_2), 2.29 (s, 3H, CH_3) 1.85–1.78 (m, 2H, CH_2) ppm; ^{13}C NMR (101 MHz, DMSO-d_6): δ 194.6 (CH_2C=O), 155.4 (C-5), 154.1 (C=O), 150.2 (C=O), 148.7 (NCN), 134.5 (C-1), 133.0 (C-3), 129.2 (C-2), 128.0 (C_{Br}), 119.7 (C-4), 115.5 (C-6), 109.0 (NCC=O), 58.5 (OCH_2), 54.3 (CH_2C=O), 38.7 (NCH_2), 31.0 (CH_2), 19.8 (CH_3) ppm; MS (ESI+): *m*/*z* 461 (M + Na, ^{81}Br, 25%), 459 (M^+ + Na, ^{79}Br, 23), 439 (M^+ + H, ^{81}Br, 100), 437 (M + H, ^{79}Br, 97).

7-(5-Hydroxy-2-methylphenyl)-1-(3-hydroxypropyl)-8-(2-methoxyphenyl)-1*H*-imidazo[2,1-*f*]purine-2,4(3*H*,8*H*)-dione (13a). Compound **11d** (1.15 g, 2.64 mmol), 2-methoxyaniline (**12a**, 5.8 mL, 52.8 mmol) and $AlCl_3$ (anhydrous, 393 mg, 2.95 mmol) were dissolved in absolute EtOH (40 mL) and the mixture was heated at 175 °C for 3 d in a high pressure reactor (quarz glass tube). Afterwards, the solvent was removed and the crude product was purified by column chromatography (ethyl acetate → ethyl acetate : MeOH 20 : 1) to obtain **13a** as a greyish solid (730 mg, 62%); mp 282–283 °C; R_f = 0.32 (ethyl acetate : MeOH = 10 : 1); ^{1}H NMR (400 MHz, DMSO-d_6): δ 10.97 (s, 1H, NH), 9.73 (s, 1H, HOPh), 7.74 (s, 1H, CH), 7.42–7.37 (m, 2H, H-4′, H-6′), 7.12 (d, $^3J_{3,4}$ = 8.3 Hz, H-3), 7.00–6.97 (m, 2H, H-3′,5′), 6.62 (dd, $^3J_{3,4}$ = 8.3 Hz, $^4J_{4,6}$ = 2.5 Hz, 1H, H-4), 6.55 (d, $^4J_{4,6}$ = 2.5 Hz, 1H, H-6), 4.45 (t, ^3J = 5.4 Hz, 1H, OH), 3.92 (t, ^3J = 7.1 Hz, 2H, NCH_2), 3.62 (s, 3H, OCH_3), 3.41 (dt, $^3J_{H,H}$ = 6.1 Hz, $^3J_{H,OH}$ = 5.4 Hz, 2H, $HOCH_2$), 2.11 (s, 3H, CH_3), 1.80–1.74 (m, 2H, CH_2) ppm; ^{13}C NMR (101 MHz, DMSO-d_6): δ 154.7 (C-2′), 154.5 (C=O), 153.4 (C-5), 152.4 (C_q), 150.8 (C=O), 147.3 (NCN), 131.8 (C=CPh), 130.9 (C-3), 130.8 (C-4′), 129.5 (C-5′), 127.8 (C-1), 127.7 (C-1′), 122.3 (C-2), 120.7 (C-6′), 117.9 (C-4), 116.3 (C-3′), 112.8 (C-6), 106.3 (CH), 99.1 (NCC=O), 58.4 (OCH_2), 55.6 (OCH_3), 38.7 (NCH_2), 30.9 (CH_2), 18.7 (CH_3) ppm; MS (ESI+): *m*/*z* 484 (M^+ + Na, 100%), 462 (M + H, 45).

7-(5-Hydroxy-2-methylphenyl)-8-(2-(3-hydroxypropoxy)phenyl)-1-methyl-1*H*-imidazo[2,1-*f*]purine-2,4(3*H*,8*H*)-dione (13b). Compound **11c** (500 mg, 1.27 mmol), 2-(3-hydroxy(propoxy)) aniline (**12b**, 1.81 g, 10.82 mmol) and $AlCl_3$ (anhydrous, 393 mg, 2.95 mmol) were dissolved in absolute EtOH (20 mL) and the mixture was heated at 175 °C for 3 d in a high pressure reactor (quarz glass tube). Afterwards, the solvent was removed and the crude product was purified by column chromatography ($CHCl_3$: EtOH 15 : 1). Afterwards, the resulting solid was washed with ethyl acetate to obtain **13b** as a greyish solid (326 mg, 56%); R_f = 0.45 ($CHCl_3$: MeOH = 5 : 1); ^{1}H NMR (400 MHz, DMSO-d_6): δ 0.97 (s, 1H, 1-NH), 9.25 (s, 1H, PhOH), 7.74 (s, 1H, CH), 7.39 (dt, ^3J = 8.0 Hz, ^4J = 1.7 Hz, 1H, H-4′), 7.32 (dd, ^3J = 7.7 Hz, ^4J = 1.7 Hz, 1H, H-6′), 7.14 (dd, ^3J = 8.5 Hz, ^4J = 1.2 Hz, 1H, H-3′), 6.95–6.99 (m, 2H, H-3, H-5′), 6.63 (dd, $^3J_{3,4}$ = 8.3 Hz, $^4J_{4,6}$ = 2.6 Hz, 1H, H-4), 6.59 (d, $^4J_{4,6}$ = 2.6 Hz, 1H, H-6), 4.41 (t, ^3J = 5.1 Hz, 1H, OH), 3.91–4.04 (m, 2H, OCH_2), 3.28–3.34 (m, 5H, CH_2OH, NCH_3), 2.10 (s, 3H, $PhCH_3$), 1.71–1.61 (m, 2H, CH_2) ppm; ^{13}C NMR (101 MHz, DMSO-d_6): δ 154.6 (C_q), 154.2 (C=O), 153.4 (C_q), 153.0 (C_q), 151.1 (C=O), 147.6 (NCN), 131.8 (C-1), 130.9 (C-3), 130.8 (C-4′), 129.7 (C-6′), 127.8 (C_q), 127.6 (C_q), 122.4 (C_q), 120.4 (C_q), 117.9 (C-6), 116.3 (C-4), 113.3 (C-3′), 106.4 (CH_{Ar}), 99.1 (NCC=O), 65.3 (OCH_2), 57.1 (CH_2OH), 31.8 (CH_2), 28.8, 18.8 (2 × CH_3); MS (ESI+): *m*/*z* 484 (M^+ + Na, 100%), 462 (M + H, 60).

4-Methyl-3-(1-methyl-2,4-dioxo-8-(2-(3-(tosyloxy)propoxy)phenyl)-2,3,4,8-tetrahydro-1*H*-imidazo[2,1-*f*]purin-7-yl)phenyl 4-methylbenzenesulfonate (14a). Compound **13b** (250 mg, 0.54 mmol) was dissolved in anhydrous *N*-methyl morpholine (5 mL), tosyl chloride (437 mg, 2.29 mmol) was added and the mixture was allowed to stirr at rt overnight. Water was added to the reaction mixture, the precipitate was filtered off and purified *via* column chromatography (petroleum ether : ethyl acetate 1 : 5) to obtain **14a** as a pale yellow solid (400 mg, 96%); R_f = 0.79 ($CHCl_3$: MeOH = 10 : 1); ^{1}H NMR (400 MHz, DMSO-d_6): δ 11.01 (s, 1H, NH), 7.82 (s, 1H, CH), 7.62 (d, ^3J = 8.3 Hz, 2H, Ts-H_{ortho}), 7.51 (d, ^3J = 8.5 Hz, 2H, Ts-H_{ortho}), 7.45–7.35 (m, 4, Ts-H_{meta}), 7.39 (d, ^3J = 8.0 Hz, 2H, PhOTs-H_{meta}), 7.32 (d, ^3J = 8.1 Hz, 2H, H_{meta}), 7.14 (dd, ^3J = 7.9 Hz, ^4J = 1.5 Hz, 1H, H-3′), 7.16–7.08 (m, 2H, H-3′,5′), 6.97–6.99 (m, 2H, H-3, H-6), 6.77 (dd, $^3J_{3,4}$ = 8.3 Hz, $^4J_{4,6}$ = 2.5 Hz, 1H, H-4), 3.99–3.86 (m, 4H, OCH_2 + NCH_2), 3.29 (s, 3H, NCH_3), 2.41 (s, 3H, Me_{Ts}), 2.36 (s, 3H, Me_{Ts}), 2.11 (s, 3H, CH_3), 1.91–1.68 (m, 2H, CH_2) ppm; ^{13}C NMR (101 MHz, DMSO-d_6): δ 153.7, 153.5, 152.9, 151.1, 147.5, 146.4, 145.8, 144.8, 137.3, 132.4 (2 × C=O + 8 × C_{Ar}), 131.5, 131.0 (2 × CH_{Ar}), 130.9 (CH_{Ar}), 130.1, 130.0 (2 × Ts-m), 129.8 (C_{Ar}), 129.6 (CH_{Ar}), 128.6 (C_{Ar}), 128.2, 127.2 (2 × Ts-o), 113.5 (C-6), 107.2 (CH), 99.2 (NCC=O), 67.6, 63.9 (CH_2), 28.8 (NCH_3), 28.0 (CH_2), 21.1, 21.0 (2 × $TsCH_3$), 19.0 (CH_3) ppm; MS (ESI+): *m*/*z* 770 (M^+ + H, 90%), 598 (M − OTs, 15).

3-(8-(2-Methoxyphenyl)-2,4-dioxo-1-(3-(tosyloxy)propyl)-2,3,4,8-tetrahydro-1*H*-imidazo[2,1-*f*]purin-7-yl)-4-methylphenyl 4-methylbenzenesulfonate (14b). Compound **13a** (200 mg, 0.44 mmol) was dissolved in anhydrous *N*-methyl morpholine (5 mL), tosyl chloride (350 mg, 1.84 mmol) was added and the mixture was allowed to stirr at rt overnight. Water was added to the reaction

mixture, the precipitate was filtered off and purified *via* column chromatography (petroleum ether : ethyl acetate 1 : 5) to obtain **14b** as a pale yellow solid (260 mg, 77%); mp 89–90 °C; R_f = 0.71 ($CHCl_3$: MeOH = 10 : 1); ^{1}H NMR (400 MHz, DMSO-d_6): δ 10.95 (s, 1H, NH), 7.79 (s, 1H, CH), 7.64 (d, ^3J = 8.3 Hz, 2H, H_{ortho}), 7.48 (d, ^3J = 8.4 Hz, 2H, PhOTs-H_{ortho}), 7.46–7.43 (m, 1H, H-6′), 7.39 (d, ^3J = 8.0 Hz, 2H, PhOTs-H_{meta}), 7.32 (d, ^3J = 8.1 Hz, 2H, H_{meta}), 7.31–7.29 (m, 1H, H-4′), 7.16–7.10 (m, 2H, H-3′,5′), 6.98 (dt, $^3J_{3,4}$ = 8.0 Hz, $^5J_{3,6}$ = 0.9 Hz, H-3), 6.88 (d, $^3J_{4,6}$ = 2.6 Hz, 1H, H-6), 6.73 (dd, $^3J_{3,4}$ = 8.0 Hz, $^4J_{4,6}$ = 2.6 Hz, 1H, H-4), 4.01 (t, ^3J = 6.3 Hz, 1H, $TsOCH_2$), 3.83 (t, ^3J = 6.5 Hz, 2H, NCH_2), 3.54 (s, 3H, OCH_3), 2.36 (s, 3H, PhOTs-CH_3), 2.35 (s, 3H, $TsCH_3$), 2.18 (s, 3H, CH_3), 1.93–1.90 (m, 2H, CH_2) ppm; ^{13}C NMR (101 MHz, CD_3CN): δ 156.0 (C-2′), 154.2 (C=O), 154.0 (C-5), 151.9 ($C(N)_3$), 148.9 (C=O), 147.9 (NCN), 147.3 ($PhTsO_{para}$), 146.3 (TsO_{para}), 138.9 (C-1), 132.6 (C=CPh), 132.3 ($PhTsO_{ipso}$, TsO_{ipso}), 131.6 (C-3), 131.0 ($PhTsO_{meta}$), 130.9 (TsO_{meta}), 130.5 (C-5′), 130.0 (C-2), 129.3 ($PhTsO_{ortho}$), 129.2 (C-4′), 128.6 (TsO_{ortho}), 126.6 (C-5′), 125.9 (C-1′), 124.0 (C-4), 123.2 (C-6′), 121.8 (C-3′), 113.7 (C-6), 107.9 (CH), 100.6 (NCC=O), 69.6 (OCH_2), 56.4 (OCH_3), 40.3 (NCH_2), 28.2 (NCH_2CH_2), 21.7 ($TsOCH_3$), 19.8 (CH_3) ppm; MS (ESI+): *m*/*z* 770 (M^+ + H, 90%), 598 (M − OTs, 15).

1-(3-Fluoropropyl)-7-(5-hydroxy-2-methylphenyl)-8-(2-methoxyphenyl)-1*H*-imidazo[2,1-*f*]purine-2,4(3*H*,8*H*)-dione (3). Compound **13a** (150 mg, 0.33 mmol) was dissolved in a mixtrue of *N*-methyl morpholine (5 mL) and DCM (5 mL). The reaction mixture was cooled to −78 °C and DAST (200 μL, 1.51 mmol) was added stepwise. After complete addition the reaction mixture was stirred at rt overnight. Afterwards, ice was added, and the aqueous phase extracted with $CHCl_3$ (3 × 20 mL). The combined organic layers were washed with saturated hydrogen carbonate solution (20 mL) and water (20 mL). The crude product was purified by column chromatography ($CHCl_3$ → $CHCl_3$: MeOH 30 : 1 → 20 : 1 → 10 : 1) to obtain **3** as pale yellow solid (30 mg, 10%); mp 194–195 °C; R_f = 0.37 ($CHCl_3$: MeOH = 9 : 1); ^{1}H NMR (400 MHz, DMSO-d_6): δ 9.23 (s, 1H, HOPh), 7.74 (s, 1H, CH), 7.41–7.37 (m, 2H, H-4′,6′), 7.12 (dd, $^3J_{3,4}$ = 8.0 Hz, $^4J_{3,6}$ = 1.7 Hz, 1H, H-3), 7.02–6.97 (m, 2H, H-3′,5′), 6.61 (dd, $^3J_{3,4}$ = 8.0 Hz, $^4J_{4,6}$ = 2.7 Hz, 1H, H-4), 6.54 (d, $^4J_{4,6}$ = 2.7 Hz, 1H, H-6), 4.48 (dt, $^3J_{H,F}$ = 47.3 Hz, $^3J_{H,H}$ = 5.8 Hz, 2H, FCH_2), 3.96 (t, ^3J = 6.2 Hz, 2H, NCH_2), 3.64 (s, 3H, OCH_3), 2.11 (s, 3H, CH_3), 1.94–1.93 (m, 2H, CH_2) ppm; ^{13}C NMR (101 MHz, DMSO-d_6): δ 154.7 (C_q), 154.5 (C=O), 153.5 (C_q), 152.3 (C_q), 150.8 (C=O), 147.3 (NCN), 131.8 (C-1), 130.8 (C-3), 130.7 (C-4′), 129.5 (C-6′), 127.9 (C_q), 127.7 (C_q), 122.3 (C_q), 120.7 (C_q), 117.9 (C-6), 116.3 (C-4), 112.8 (C-3′), 106.3 (CH_{Hetar}), 99.2 (NCC=O), 79.5 ($^1J_{C,F}$ = 163.1 Hz, CH_2F), 63.8 ($^3J_{C,F}$ = 5.8 Hz, OCH_2), 29.5 (d, $^2J_{C,F}$ = 19.5 Hz, CH_2), 30.8, 18.7 (2 × CH_3) ppm; ^{19}F NMR (376 MHz, DMSO-d_6): δ −218.3 ppm; MS (ESI+): *m*/*z* 464 (M^+ + H, 10%).

8-(2-(3-Fluoropropoxy)phenyl)-7-(5-hydroxy-2-methylphenyl)-1-methyl-1*H*-imidazo[2,1-*f*]purine-2,4(3*H*,8*H*)-dione (2). Compound **13b** (100 mg, 0.22 mmol) was suspended in anhydrous THF (5 mL) and deoxofluor (300 μL, 1.6 mmol) was added. After stirring at rt for 1.5 h, water (25 mL) was added and the aqueous solution extracted with ethyl acetate (3 × 20 mL). The crude product was purified by column chromatography (CH_2Cl_2 : EtOH = 30 : 1) to give **1b** as a greyish solid (80 mg, 80%); mp 308 °C; R_f = 0.60 ($CHCl_3$: EtOH = 5 : 1); ^{1}H NMR (400 MHz, DMSO-d_6): δ 10.99 (s, 1H, NH), 9.27 (s, 1H, HOPh), 7.76 (s, 1H, CH), 7.40 (dt, ^3J = 7.9 Hz, ^4J = 1.6 Hz, 1H, H-4′), 7.30 (dd, ^3J = 7.8 Hz, ^4J = 1.6 Hz, 1H, H-6′), 7.19 (dd, ^3J = 8.5 Hz, ^4J = 1.1 Hz, 1H, H-3′), 6.96–7.00 (m, 2H, H-3, H-5′), 6.64 (dd, $^3J_{3,4}$ = 8.3 Hz, $^4J_{4,6}$ = 2.6 Hz, 1H, H-4), 6.59 (d, $^4J_{4,6}$ = 2.6 Hz, 1H, H-6), 4.39–4.28 (m, 2H, CH_2F), 3.98–4.09 (m, 2H, OCH_2), 3.32 (s, 3H, NCH_3), 2.09 (s, 3H, $PhCH_3$), 2.00–1.81 (m, 2H, CH_2) ppm; ^{13}C NMR (101 MHz, DMSO-d_6): δ 154.6 (C_q), 153.9 (C=O), 153.4 (C_q), 152.8 (C_q), 151.0 (C=O), 147.5 (NCN), 131.7 (C-1), 130.9 (C-3), 130.8 (C-4′), 129.7 (C-6′), 127.8 (C_q), 127.6 (C_q), 122.5 (C_q), 120.7 (C_q), 117.9 (C-6), 116.3 (C-4), 113.4 (C-3′), 106.5 (CH_{Hetar}), 99.1 (NCC=O), 80.4 ($^1J_{C,F}$ = 162.4 Hz, CH_2F), 64.0 ($^3J_{C,F}$ = 5.5 Hz, OCH_2), 29.5 (d, $^2J_{C,F}$ = 19.5 Hz, CH_2), 28.8, 18.7 (2 × CH_3) ppm; ^{19}F NMR (376 MHz, DMSO-d_6): δ −220.7 ppm; MS (ESI+): *m*/*z* 486 (M^+ + Na, 100%), 464 (M^+ + H, 30).

8-(2-(3-[^{18}F]Fluoropropoxy)phenyl)-7-(5-hydroxy-2-methylphenyl)-1-methyl-1*H*-imidazo[2,1-*f*]purine-2,4(3*H*,8*H*)-dione ([^{18}F]2). An anion-exchange cartridge (Waters, Sep-Pak Light Accell Plus QMA) was activated by rinsing with 5 mL of a 1 M $NaHCO_3$ solution and 10 mL of deionised H_2O. It was charged with [^{18}F]fluoride (2–3 GBq) and eluted with 1.5 mL of a solution of Kryptofix 2.2.2 (10 mg mL^{-1}) and K_2CO_3 (13 mM) in 7 mL CH_3CN and 43 mL H_2O. The solvents were evaporated azeotropically by subsequent addition of three portions of 1 mL each of anhydrous CH_3CN under a stream of nitrogen at 110 °C. Precursor **14a** (approx. 3 mg) was dissolved in 500 μL of anhydrous CH_3CN and the mixture was added to the [^{18}F] fluoride-containing sealed vial. The resulting solution was heated at 100 °C for 30 min. Afterwards, aqueous NaOH (40 μL, 5 M) was added and the mixture heated at 100 °C for 15 min. After cooling to rt, 120 μL of water were added and the solution purified by semi-preparative radio-HPLC (peak collection t_R: 24–28 min, gradient: 60% water, 40% CH_3CN + 0.1% TFA). To remove the solvent from the product, the solvent of the collected product fraction was removed under reduced pressure. Analytical radio-HPLC: t_R = 12.0 min; RCY: 57–129 MBq (3–5%, d.c.); RCP: >98%; A_m = 11.6 ± 3.4 GBq μmol^{-1}.

1-(3-[^{18}F]Fluoropropyl)-7-(5-hydroxy-2-methylphenyl)-8-(2-methoxyphenyl)-1*H*-imidazo[2,1-*f*]purine-2,4(3*H*,8*H*)-dione ([^{18}F]3). An anion-exchange cartridge (Waters, Sep-Pak Light Accell Plus QMA) was activated by rinsing with 5 mL of a 1 M $NaHCO_3$ solution and 10 mL of deionised H_2O. It was charged with [^{18}F]fluoride (~2 GBq) and eluted with 1.5 mL of a solution of Kryptofix 2.2.2 (10 mg mL^{-1}) and K_2CO_3 (13 mM) in 7 mL CH_3CN and 43 mL H_2O. The solvents were evaporated azeotropically by subsequent addition of three portions of 1 mL each of anhydrous CH_3CN under a stream of nitrogen at 110 °C. Precursor **14b** (approx. 3 mg) was dissolved in 300 μL of anhydrous CH_3CN and the mixture was added to the [^{18}F] fluoride-containing sealed vial. The resulting solution was heated under microwave conditions at 50 watt for 70 min. After cooling to rt, 3 mL of water were added and the solution

transferred to 2 connected Chromafix C18 ec-cartridges. The cartridges were washed with 20 mL of water and the tracer eluted with 0.9 mL of MeOH. Further purification was done *via* semi-preparative radio-HPLC (peak collection t_R: 9–11 min). To remove the solvent from the product, the solvent of the collected product fraction was removed under reduced pressure. Analytical radio-HPLC: t_R = 15.2 min; RCY: 21–69 MBq (1–6%, d.c.); RCP: >98%; A_m = 10.3 ± 5.1 GBq μmol^{-1}.

Biological characterisation

Generation of EphA2- and EphB4-transgenic A375 cells. Human A375 melanoma cells overexpressing EphA2 or EphB4 were prepared as described previously by us.[28,48] In brief, A375 cells were stably transfected with a plasmid encoding for both the reporter green fluorescent protein (GFP) and the EphA2 (A375-EphA2) or EphB4 receptor (A375-EphB4). GFP expression was used to select transfected cells by fluorescence associated cell sorting (FACS) and to routinely control stable expression of EphA2 and EphB4.

Verification of EphA2- and EphB4-overexpression. Enhanced EphA2- and EphB4-expression in A375-EphA2 and A375-EphB4 cells, respectively, was verified by Western blot as described previously.[28,48]

Cellular binding and uptake studies and blocking experiments. Cellular binding and uptake of the radiotracers [^{18}F]**2** and [^{18}F]**3** were investigated in A375, A375-EphA2, and A375-EphB4 cells for up to 120 min as previously described by us.[28] For blocking experiments, cellular binding and uptake of [^{18}F]**2** and [^{18}F]**3** was investigated after pre-incubation with compound **2** for 30 min and lead compound **1** for 10 min, respectively. Cellular binding and uptake was investigated in at least two independent experiments, each performed in quadruplicate.

***In vitro* stability test.** The *in vitro* stability was investigated using rat blood or plasma. Thus, purified [^{18}F]**2** or [^{18}F]**3** was diluted in 200 μL E153 infusion solution and then incubated with 3 mL of rat blood or plasma for 60 min at 37 °C. Samples were taken after time points of 1, 30 and 60 min, and analysed by radio-TLC (silica gel, eluent: chloroform : methanol 9 : 1).

Animal experiments. For *in vivo* stability tests, radiotracers [^{18}F]**2** and [^{18}F]**3** were injected i.v. into male Wistar rats (body weight approx. 236 g, injected dose approx. 10 MBq) under desflurane anesthesia (10% desflurane in 30% oxygen/air). Using a catheter, blood samples from femoral artery were taken at 1, 3, 5, 10, 20, 30, and 60 min p.i. The resulting loss of volume was compensated by i.v. injection of E153. All animal experiments were carried out according to the guidelines of the German Regulations for Animal Welfare. The protocols were approved by the local Ethical Committee for Animal Experiments (AZ 24-9168.21-4/2004-1 and 24-9168.11-4/2012-1).

Conclusions

Two novel fluorine-18-containing radiotracers based on the xanthine lead structure were prepared and characterised to target selected human Eph receptors. Docking studies were done to find suitable positions on the original inhibitor for a radiolabelling with fluorine-18. Two positions were figured out and the respective non-radioactive references and precursors prepared followed by a straightforward radiolabelling procedure with [^{18}F]fluoride with radiochemical yields between 3–15% and radiochemical purity >95% for [^{18}F]**2/3**.

First radiobiological studies were done *in vitro* on human A375 melanoma cells showing a low uptake for [^{18}F]**2** (approx. 40% ID mg^{-1}) and a substantial uptake for [^{18}F]**3** (60–110% ID mg^{-1}), but nearly no difference between the transfected A375-EphA2 and A375-EphB4 cells compared to the non-transfected A375 cells.

In vivo investigations showed a fast blood clearance and a metabolisation of the radiotracers to a more lipophilic compound in the urine after 60 min p.i., but no radiodefluorination.

Conflicts of interest

There are no conflicts to declare.

Acknowledgements

The authors are grateful to Jaques Pliquett, Waldemar Herzog, Stephan Preusche, and Tilow Krauss for their excellent technical and laboratory assistance. We are very thankful to Andrea Suhr, Catharina Heinig, and Regina Herrlich for the *in vitro* and *in vivo* experiments. This work is part of a research initiative within the Helmholtz-Portfoliothema "Technologie und Medizin – Multimodale Bildgebung zur Aufklärung des *In vivo*-Verhaltens von polymeren Biomaterialien".

Notes and references

1 B. Mosch, B. Reissenweber, C. Neuber and J. Pietzsch, *J. Oncol.*, 2010, 135285.
2 L.-Y. Liang, O. Patel, P. W. Janes, J. M. Murphy and I. S. Lucet, *Oncogene*, 2019, **38**, 6567.
3 J. G. Flanagan and P. Vanderhaeghen, *Annu. Rev. Neurosci.*, 1998, **21**, 309.
4 N. Cheng, D. M. Brantley and J. Chen, *Cytokine Growth Factor Rev.*, 2002, **13**, 75.
5 E. B. Pasquale, *Cell*, 2008, **133**, 38.
6 C. Zhao, N. Irie, Y. Takada, K. Shimoda, T. Miyamoto, T. Nishiwaki, T. Suda and K. Matsuo, *Cell Metab.*, 2006, **4**, 111.
7 E. B. Pasquale, *Nat. Rev. Mol. Cell Biol.*, 2005, **6**, 462.
8 J. Chen, *Adv. Cancer Res.*, 2012, **114**, 1.
9 N. K. Noren and E. B. Pasquale, *Cancer Res.*, 2007, **67**, 3994.
10 J. E. Lisle, I. Mertens-Walker, R. Rutkowski, A. C. Herington and S.-A. Stephenson, *Biochim. Biophys. Acta*, 2013, **1835**, 243.
11 X. Yang, Y. Yang, S. Tang, H. Tang, G. Yang, Q. Xu and J. Wu, *J. Pharmacol. Sci.*, 2015, **129**, 65.

12 I. Guijarro-Muñoz, A. Sánchez, E. Martínez-Martínez, J. M. García, C. Salas, M. Provencio, L. Alvarez-Vallina and L. Sanz, *Med. Oncol.*, 2013, **30**, 572.
13 J. Wykosky and W. Debinski, *Mol. Cancer Res.*, 2008, **6**, 1795.
14 N. K. Noren, M. Lu, A. L. Freeman, M. Koolpe and E. B. Pasquale, *Proc. Natl. Acad. Sci. U. S. A.*, 2004, **101**, 5583.
15 J. H. Lv, Q. Y. Xia, J. J. Wang, Q. Shen, J. Zhang and X. J. Zhou, *Exp. Mol. Pathol.*, 2016, **100**, 402.
16 C. Neuber, B. Belter, S. Meister, F. Hofheinz, R. Bergmann, H.-J. Pietzsch and J. Pietzsch, *Molecules*, 2018, **23**, 444.
17 X. Yang, Y. Yang, S. Tang, H. Tang, G. Yang, Q. Xu and J. Wu, *J. Pharmacol. Sci.*, 2015, **129**, 65.
18 I. Guijarro-Muñoz, A. Sánchez, E. Martínez-Martínez, J. M. García, C. Salas, M. Provencio, L. Alvarez-Vallina and L. Sanz, *Med. Oncol.*, 2013, **30**, 572.
19 M. Koolpe, M. Dail and E. B. Pasquale, *J. Biol. Chem.*, 2002, **277**, 46974.
20 J. E. Chrencik, A. Brooun, M. I. Recht, G. Nicola, L. Davis, R. Abagyan, H. Widmer, E. B. Pasquale and P. Kuhn, *J. Biol. Chem.*, 2007, **282**, 36505.
21 B. Ma, S. Kolb, M. Diprima, M. Karna, G. Tosato, Q. Yang, Q. Huang and R. Nussinov, *Growth Factors*, 2014, **32**, 236.
22 R. Noberini, I. Lamberto and E. B. Pasquale, *Semin. Cell Dev. Biol.*, 2012, **23**, 51.
23 Y. Liu, X. Lan, T. Wu, J. Lang, X. Jin, X. Sun, Q. Wen and R. An, *Nucl. Med. Biol.*, 2014, **41**, 450.
24 C. Xiong, M. Huang, R. Zhang, S. Song, W. Lu, L. Flores II, J. Gelovani and C. Li, *J. Nucl. Med.*, 2011, **52**, 241.
25 M. Pretze, M. Kuchar, R. Bergmann, J. Steinbach, J. Pietzsch and C. Mamat, *ChemMedChem*, 2013, **8**, 935.
26 M. Pretze, B. Mosch, R. Bergmann, J. Steinbach, J. Pietzsch and C. Mamat, *J. Labelled Compd. Radiopharm.*, 2014, **57**, 660.
27 K. Ebert, J. Wiemer, J. Caballero, M. Köckerling, J. Steinbach, J. Pietzsch and C. Mamat, *Bioorg. Med. Chem.*, 2015, **23**, 6025.
28 C. Mamat, B. Mosch, C. Neuber, M. Köckerling, R. Bergmann and J. Pietzsch, *ChemMedChem*, 2012, **7**, 1991.
29 J. Wiemer, J. Steinbach, J. Pietzsch and C. Mamat, *J. Labelled Compd. Radiopharm.*, 2017, **60**, 489.
30 K. Lafleur, D. Huang, T. Zhou, A. Caflisch and C. Nevado, *J. Med. Chem.*, 2009, **52**, 6433.
31 K. Lafleur, J. Dong, D. Huang, A. Caflisch and C. Nevado, *J. Med. Chem.*, 2013, **56**, 84.
32 M. Pretze, D. Pietzsch and C. Mamat, *Molecules*, 2013, **18**, 8618.
33 P. Traxler and P. Furet, *Pharmacol. Ther.*, 1999, **82**, 195.
34 K. C. Lee, S.-Y. Lee, Y. S. Choe and D. Y. Chi, *Bull. Korean Chem. Soc.*, 2004, **25**, 1225.
35 M. Kuchar and C. Mamat, *Molecules*, 2015, **20**, 16186.
36 W. Kirmse, H. J. Schladetsch and H.-W. Bücking, *Chem. Ber.*, 1966, **99**, 2579.
37 W. Traube, *Ber. Dtsch. Chem. Ges.*, 1900, **33**, 3035.
38 E. Kinski, Diploma thesis, Zittau/Görlitz University of Applied Sciences, 2012.
39 M. Pretze, PhD thesis, Technical University Dresden, 2014.
40 L. S. Cai, S. Y. Lu and V. W. Pike, *Eur. J. Org. Chem.*, 2008, 2853.
41 *ChemDraw Professional, Version 17.0.0.206*, PerkinElmer Informatics Inc., 1998–2017.
42 *ACD Labs, Version 2017.2.1*, Advanced Chemistry Development Inc., 1994–2018.
43 J. W. Hicks, H. F. VanBrocklin, A. A. Wilson, S. Houle and N. Vasdev, *Molecules*, 2010, **15**, 8260.
44 J. E. van Muijlwijk-Koezen, H. Timmerman, R. P. van der Sluis, A. C. van de Stolpe, W. M. P. B. Menge, M. W. Beukers, P. H. van der Graaf, M. de Groote and A. P. IJzerman, *Bioorg. Med. Chem. Lett.*, 2001, **11**, 815.
45 A. Hagey, J. E. Lancet, V. Palath, A. H. Wei, M. Lackmann, J. E. Cortes, A. Boyd, D. Shochat, G. Yarranton, C. Bebbington and J. A. Leff, *Blood*, 2011, **118**, 4893.
46 A. W. Boyd, P. F. Bartlett and M. Lackmann, *Nat. Rev. Drug Discovery*, 2014, **13**, 39.
47 (*a*) G. M. Sheldrick, *SHELXS and SHELXL - Programs for the Solution and Refinement of Crystal Structures*, University of Göttingen, 1997; (*b*) G. M. Sheldrick, *Acta Crystallogr., Sect. A: Found. Crystallogr.*, 2008, **64**, 112.
48 B. Mosch, D. Pietzsch and J. Pietzsch, *Cell Adhes. Migr.*, 2012, **6**, 113.